Time-harmonic Eddy-current calculation with Capacitive Circuit parameters

S. Dappen and G. Henneberger
Institut für Elektrische Maschinen, RWTH Aachen, 52056 Aachen, Germany

***Abstract*—This paper presents the calculation of a time-harmonic eddy-current field in combination with capacitive circuit devices. The computation has been performed by a weak coupling of the circuit and the field equations. An incomplete solution of the system matrix and a scaling of the matrix by the new resonance frequency have been realized to accelerate the calculation process. The calculation method has been applied to the technically important resonance inverters supplying an induction furnace. The results agree well to measurements.**

I. Introduction

In the field of induction heating, oscillating circuit inverters of the serial or parallel type are state of the art. Inductive heating devices usually have large air gaps, which lead to a high demand of reactive power. In order to reduce the semiconductor costs, only the active power will be fed into a resonant circuit consisting of compensation capacitors and the heating unit. The calculation of such inverter fed systems with a time-harmonic FE approach regarding the capacitors as circuit parameters is not immediately possible since the feeding frequency of the inverter is not constant but a function of the electromagnetic device's impedance.

Although the literature concerning the coupling of circuit and electromagnetic field equations is extensive, only a few papers examine the combination with lumped capacitors. Most published methods perform a transient approach [1-3]. [4] shows the calculation of a magnetic frequency tripler in which the excitation and the field values are expressed by harmonic solutions.

Below a different approach will be suggested to solve the problem iteratively.

II. Field- and Circuit-Calculations

The weakly coupled iterative calculation procedure can be divided into the FE field computation and the calculation of the resonant circuit.

Manuscript received Juli 10, 1995.
S. Dappen, e-mail: dappen@iem.rwth-aachen.de;
G. Henneberger, e-mail: henneberger@rwth-aachen.de

A. Field Computation

The Galerkin-transformed eddy-current differential equation for the time-harmonic case

$$\sum_i A_i \cdot \int_\Omega \left(\nu\, \nabla N_i\, \nabla N_j + \mathrm{j}\omega\sigma\, N_i\, N_j\right) d\Omega + \sum_i \nabla V_i \cdot \int_\Omega \sigma\, N_i\, d\Omega = 0 \qquad (1)$$

and the equation for the total current I in a conductive region Γ

$$U = R\,I + R \sum_i \int_\Gamma \mathrm{j}\omega\sigma\, N_i\, A_i\, d\Gamma \qquad (2)$$

define the set of equations for the FE calculation with a given angular frequency ω. R means the DC-resistance of the region Γ and U its voltage. The coupling of (1) and (2) to a system of linear equations (3) is realized according to [5].

$$\begin{pmatrix} \nu\, S + \mathrm{j}\omega\sigma\, T & -\sigma\, C \\ -\sigma\, C & \dfrac{1}{\mathrm{j}\omega\, R} \end{pmatrix} \cdot \begin{pmatrix} A' \\ U \end{pmatrix} = \begin{pmatrix} 0 \\ \dfrac{I}{\mathrm{j}\omega} \end{pmatrix} \qquad (3)$$

For the axisymmetric case

$$A'_i = \frac{A_i}{r_i} \qquad (4)$$

is the used auxiliary potential. The element matrices are

$$s_{ij} = \iint \frac{2\pi}{r} \left(\frac{\partial N_i}{\partial r}\frac{\partial N_j}{\partial r} + \frac{\partial N_i}{\partial z}\frac{\partial N_j}{\partial z}\right) dr\, dz \qquad (5)$$

$$t_{ij} = \iint \frac{2\pi}{r}\, N_i\, N_j\, dr\, dz \qquad (6)$$

$$c_{ij} = \iint \frac{1}{r}\, N_i\, dr\, dz \quad . \qquad (7)$$

B. Circuit Computation

The frequency is a function of the resonant circuit equations using the capacitors and also the equivalent resistance R and inductance L of the device. These can be computed from ω_n and the voltages:

$$L = \frac{\sum U_{Im}}{\omega_n I} \qquad R = \frac{\sum U_{Re}}{I} \quad . \qquad (8)$$

The resonance condition is defined by the circuit equations and the inverter's turn-off time, which is usually capacitive. The switching angle is

$$\epsilon = \sphericalangle Z_i(\omega_{n+1}, R, L, C) \quad . \tag{9}$$

III. Iterative Procedure

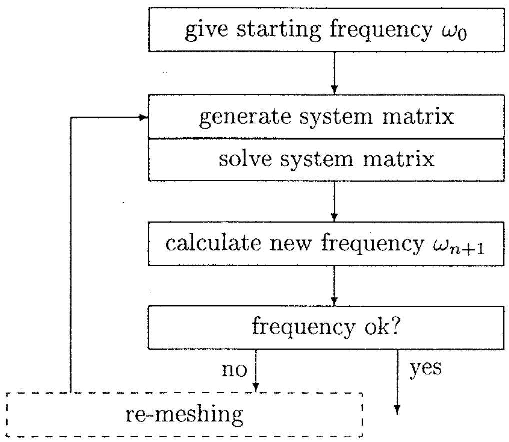

Fig. 1. Iterative procedure

The non-linear problem can be solved iteratively according to Fig. 1. Taking a given frequency ω_0 the time-harmonic field can be computed. One gets the corresponding device's impedance simply by (8). The non-linear equation (9) can be solved, giving a new frequency ω_{n+1}, which is used to compute another field problem. This weakly coupled procedure above is iterated until a given accuracy of the frequency is achieved.
A re-meshing before the next field computation is only necessary if the penetration depth has changed significantly. Starting with a mesh for the maximum allowed inverter frequency is the best choice. This iterative procedure can be performed by *any* time-harmonic FE-program.

IV. Acceleration of the Calculation Procedure

Several steps are necessary to reach the correct frequency of the resonant circuit and this can be time-consuming. With some slight alterations to a given FE code the iteration has been significantly accelerated.

A. Incomplete Solution of the FE System

Taking into account the topology of the matrix one finds that the rows, which are responsible for the total current in each conductor, usually have a lot more non-zero entries than the rest of the matrix. Therefore they show a more integrative character. Looking onto the convergence behaviour of the unknown voltages a sufficient accuracy

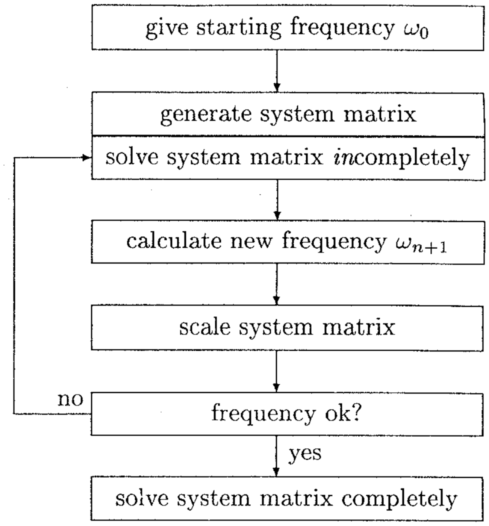

Fig. 2. Accelerated iterative procedure

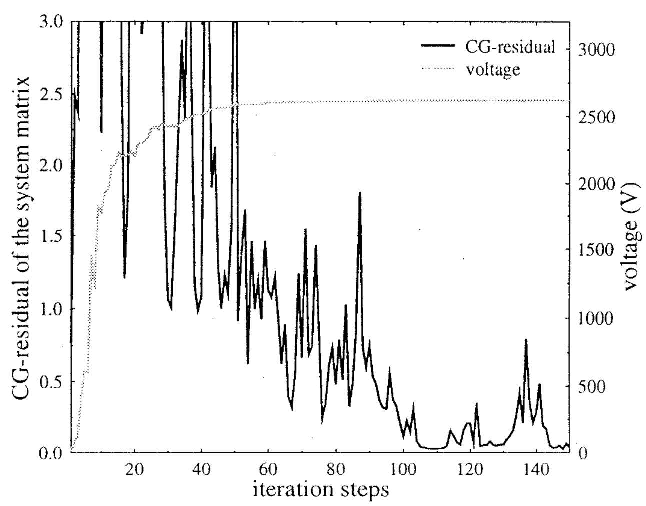

Fig. 3. CG-residual and device voltage

is reached with fewer oscillations in a faster time than for the whole solution vector (Fig. 3). The following calculation of the new supply-frequency by (9) will reduce the error even more.
Taking the voltages seems to be a good stopping criterion for the CG-procedure before the whole system matrix is correctly solved. The disadvantage is, that the voltage value at the end of the solution process is unknown during the computation, that means one could only compute the correct voltage residual after a successive matrix solution (post-solution voltage-residual).
Good results have been achieved by using the ratio between the variance of the calculated voltages of the last k CG-steps and their mean value $\bar{U}$ as the stopping criterion

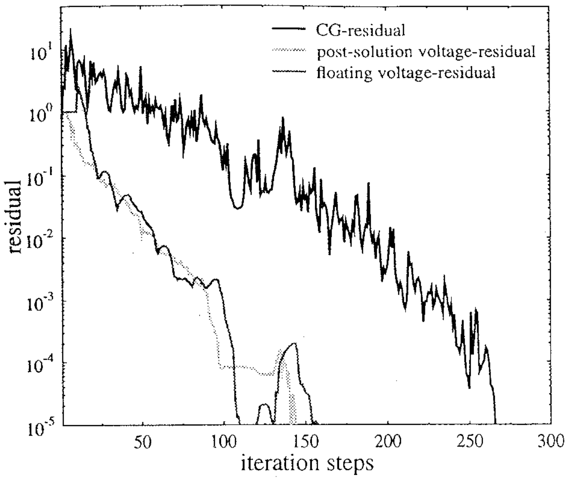

Fig. 4. Residuals for field solution and for voltage

(ρ_{float}, floating voltage-residual) for the CG-iteration.

$$\rho_{\text{float}} = \frac{1}{\bar{U}} \sqrt{\frac{1}{n-1} \sum_i (U_i - \bar{U})^2} \tag{10}$$

Fig. 4 shows the residuals for the solution vector and the two voltage-residuals which are related closely.

B. Scaling of the System Matrix

If no re-meshing from one iteration step to the next is necessary, the topology of the system matrix is unchanged. Taking a closer look on (3) shows that the system matrix starting from the second iteration step only needs a scaling to the new frequency ω_{n+1} instead of rebuilding the matrix. The scaling concerns the imaginary part of the A'-submatrix, the main diagonal of the U-submatrix

$$\begin{pmatrix} \nu\, S + \dfrac{\omega_{n+1}}{\omega_n} \mathrm{j}\omega_n \sigma\, T & -\sigma\, C \\ -\sigma\, C & \dfrac{\omega_n}{\omega_{n+1}} \dfrac{1}{\mathrm{j}\omega_n R} \end{pmatrix} \tag{11}$$

and the excitation vector

$$\begin{pmatrix} 0 \\ \dfrac{\omega_n}{\omega_{n+1}} \dfrac{I}{\mathrm{j}\omega_n} \end{pmatrix} \quad . \tag{12}$$

V. Application to the Calculation of an Induction Furnace supplied by an Oscillating Circuit Inverter

Fig. 5 shows a 4000 kg steel induction furnace supplied by an oscillating circuit inverter of the parallel type. In Fig. 6 a measured discharging period of this induction furnace is shown. During a few short periods the melt is heated to compensate the thermal losses and keep it in

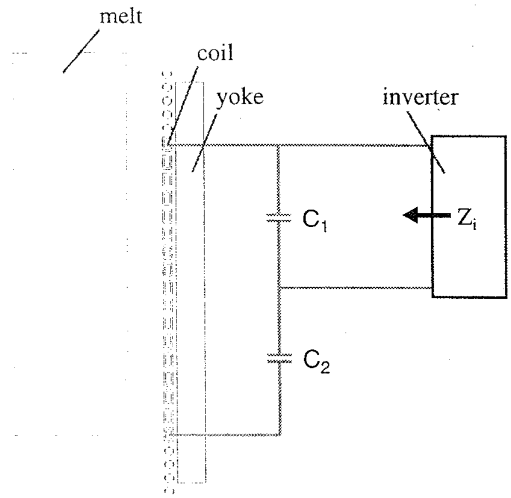

Fig. 5. Outline of the FE-model and the resonant circuit

a defined temperature range. Throughout the emptying process the frequency declines while the inductance is increasing.

Only the discharging periods were observed because they allow a description of the crucible's contents by a homogeneous material with known material parameters of a nearly constant temperature. 21 discharging processes with 214 heating periods were analysed. Fig. 7 shows the measured values. Different shaded dots mark heating intervals of different charges. Depending on the condition of the furnace, where the continuous fluid flow of the melt erodes the crucible, two sets of axisymmetric calculations were made for the extreme values of the crucible's thickness. Here the erosion of the crucible for the upper curve was assumed to be constant over the whole crucible height. The phase angle of the inverter output impedance Z_i is $\epsilon \approx -20°$. The calculations show a good agreement to the measurements (Fig. 7). The combination of the two acceleration methods achieves an average speed-up of about 40 %.

A. Numerical example

As an example for the efficiency of the above mentioned procedure the field for a melt mass of 1200 kg is computed. The parameters are

- 7325 first order elements
- starting frequency 300 Hz
- final frequency error 0.5 Hz
- CG-stopping-residual $\rho_{\text{CG}} = 0.00001$
- floating voltage-stopping-residual $\rho_{\text{float}} = 0.0001$

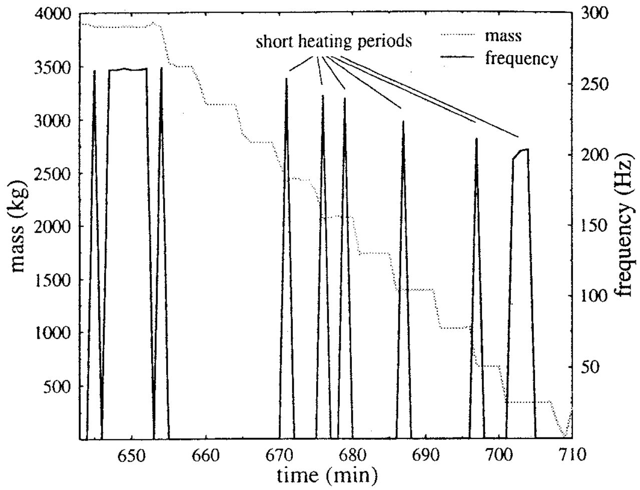

Fig. 6. Discharging process of the furnace and corresponding frequency characteristic

- averaging over $k = 10$ CG-steps

Comparing the solution times a speed-up of 39.9 % was achieved.

Number of frequency iterations	4
Simple iteration process	263.4 s
Acceleration by incomplete solution	186.1 s
Acceleration by incomplete solution and scaling of the system matrix	158.3 s
Maximum speed-up	39.9 %

VI. Conclusions

This paper presents an eddy-current field calculation with capacitive circuit parameters by a time-harmonic approach. The field and circuit equations are weakly coupled and solved iteratively. The calculation process has been accelerated significantly by the implementation of the

- incomplete solution of the system matrix using a floating voltage-residual and the
- scaling of the system matrix by the new frequency

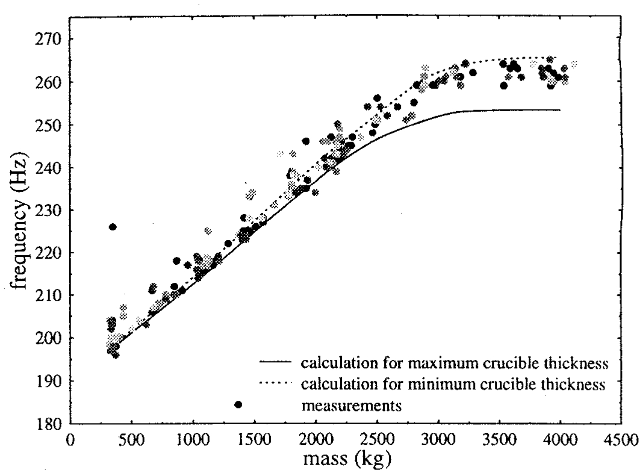

Fig. 7. Comparison of calculated and measured frequencies

in a given FE-code. The results obtained from the application of the calculation to an inverter fed induction furnace agree well to measurements.

References

[1] D. Shen, G. Meunier, J.L. Coulomb, J.C. Sabonnadiere, "Solution of magnetic fields and electric circuits combined problems", *IEEE Trans. Magn.*, vol. 21, no 6, pp. 2288-2291, November 1985.

[2] H. Haas, F. Schmoellebeck, "A finite-element method for transient skin effect in 2-D loaded multiconductor systems", *IEEE Trans. Magn.*, vol. 24, no 1, pp. 174-177, January 1988.

[3] R.H. Vander Heiden, A.A. Arkadan, J.R. Brauer, G.T. Hummert, "Finite element modeling of a transformer feeding a rectified load: the coupled power electronics and nonlinear magnetic field problem", *IEEE Trans. Magn.*, vol. 27, no 6, pp. 5217-5220, November 1991.

[4] J. Lu, S. Yamada, K. Bessho, "Harmonic balancing finite element method taking account of external circuits and motion", *IEEE Trans. Magn.*, vol. 27, no 5, pp. 4024-4027, September 1991.

[5] T. Nakata, N. Takahashi, K. Fujiwara, "Efficient solving techniques of matrix equations for finite element analysis of eddy currents", *IEEE Trans. Magn.*, Vol. 24, No.1, pp. 170-173, 1988.